Investigation of Growth Parameter Influence on Hydrothermally Grown ZnO Nanowires Using a Research Grade Microwave

Ashley D. Mason[1], Tyler F. Roberts[1], John F. Conley Jr. [1], David T. Price[2],
Derryl D. J. Allman[2], and Michael S. McGuire[2]
[1]School of Electrical and Computer Engineering, Oregon State University,
Corvallis, OR
[2]ON Semiconductor, Gresham, OR

ABSTRACT

ZnO nanowires (NWs) were grown using a research grade microwave with integrated temperature control via a hydrothermal method on a ZnO seed layer. The influences of growth time, temperature, precursor concentration and ratio, and seed layer structure on resulting NW morphology were studied using scanning electron microscopy (SEM) and x-ray diffraction (XRD). The seed layer was found to have the largest influence on NW growth. When anneals were included as part of the surface treatment prior to growth, increased crystallinity of the seed layer led to larger diameter wires. For high temperature anneals (900°C), an additional peak appeared in XRD data, which is believed to be CORRESPONDING to Zn_2SiO_4 which WAS forming at the interface between the ZnO seed layer and the Si wafer. With good process control, it was possible to grow a uniform, vertically oriented array of NWs. With a 1:1 nutrient solution of 25 mM $Zn(NO_3)_2$ and 25 mM hexamethylene tetramine (HMT), a growth temperature of 85 °C, and a growth time of 60 minutes, NWs with a length of 696 nm with ± 7% across the sample was achieved.

KEYWORDS

Zinc Oxide, Electromagnetic heating, Microwave technology, Nanotechnology, Thin films

MAIN TEXT

1. Introduction

Semiconducting nanowires have drawn much attention for their unique properties and potential applications. Nanowires made out of ZnO are of particular interest due to the unique properties of ZnO such as a wide direct bandgap, a large exciton binding energy, piezoelectric properties, and chemical sensitivity. Potential applications for ZnO nanowires include optoelectronics such as photodetectors [1-9], piezoelectric actuators and generators [2,6,10-12], UV nanolasers [3,4,6,8,12], field effect transistors [1,3,5,9,12,13], solar cell components [3,5,9,11,12,14], gas sensors [3,5,7,15], and organic filters [16]. Popular methods for growing ZnO nanowires include vapor-solid or vapor-liquid-solid (gas-phase synthesis) [2,4,9,13], and hydrothermal (solution-phase synthesis) [1,3,5,7,8,10-12,14,16] growth methods. Vapor-solid growth involves the use of nitrogen gas flowed over solid precursors to form ZnO nanowires on a catalyst-covered substrate at high temperatures, ranging from 500^{o}C to 1500^{o}C [2-

4,13,15,16]. ZnO nanowires grown in this fashion possess a highly crystalline structure and can have a high aspect ratio [4,13,15], but THE high temperatures required for this growth process pose problems for thermally-restricted fabrication processes. Hydrothermal growth methods allow for low-temperature synthesis of ZnO nanowires (NWs) directly on a variety of novel substrates required for proposed flexible substrate applications such as power-harvesting fabrics [11,16]. Although hydrothermal growth opens up a new realm of application possibilities, a major drawback of this method is THE growth time – up to 20 hours or longer have been reported as necessary to yield desired NW morphologies using conventional hot-plate heating [5,6,8,12,16]. Recently, the use of A microwave oven to supply heat to the nutrient solution has been reported to speed the growth process by Unalan, et al. [12]. Unalan, et al. reported that ZnO growth rates using microwave power were as high as 100 nm/min [12]. Traditional hydrothermal growth techniques have reported growth rates only between 100 nm/hour to 1,000 nm/hour [5,6,16]. Although growth temperature has been reported to be a critical process variable for hydrothermal growth [5][8], Unalan, et al. were not able to directly control temperature with the conventional microwave oven used in their study. Instead, indirect control of growth temperature was attempted by using different fixed settings of the microwave power level. Other conventional microwave ovens change power level through variations in duty cycle.

In this work, a research grade microwave OVEN equipped with integrated temperature control was used to systematically investigate the impact of growth temperature, growth time, solution concentration, and seed layer crystallinity on ZnO NW length, diameter, aspect ratio, growth orientation, density, and morphology. It was determined that parameters which most strongly affected THE resulting nanowire morphology were growth time and seed layer structure.

2. Experimental Details

ZnO thin films of thickness 15 nm, 90 nm, and 200 nm deposited on Si wafers were used to seed NW growth. The majority of ZnO seed layer films were deposited on 6" Si wafers via atomic layer deposition (ALD) using diethyl zinc (DEZ) and H_2O at 170°C. Prior to ZnO deposition, THE Si substrates were etched in HF to remove any native oxide film. To investigate the impact of the seed layer deposition method on NW growth, 90 nm ZnO films were also deposited via RF sputtering at 75 W and 15 mTorr Ar. 7 cm x 2 cm Si coupons were placed at a working distance of 4" from the 2" ZnO target. A select number of ALD films were annealed to investigate the impact of seed layer crystal structure on NW growth. Samples were either (i) rapid thermal annealed (RTA) in air for 10 minutes at 900°C, (ii) annealed in N_2 for 10 minutes at 900°C in a tube furnace, or (iii) annealed in N_2 for 10 minutes at 400°C in the ALD chamber.

ZnO nanowires were grown hydrothermally using $Zn(NO_3)_2$ and hexamethylene tetramine (HMT) as discussed in [7]. All NW growths were performed in a CEM Discover S Class microwave which uses a 600 W magnetron to irradiate samples and is capable of continuous operation at 300W, 300°C, and 300 psi. Microwave irradiations WERE conducted in a specially designed pressure-sealed vial. Experimental runs WERE controlled via either power, temperature, or pressure. Both temperature and pressure WERE monitored in-situ. Temperature was monitored by a vertically focused IR temperature sensor that was constructed within the microwave but outside the sealed vial. Pressure was monitored by a proprietary system that involves measuring the expansion of the flexible lid seal. Software monitors and records the system pressure, temperature, growth time, and power for each experiment.

The general procedure for microwave growth consisted of first preparing a 250 mL batch solution at the desired molarity and ratio of $Zn(NO_3)_2$ / HMT. The solution was then left stirring on a hot plate at 60 rpm at room temperature. Samples were attached to a microwave vial using Kapton tape. When the solution was thoroughly mixed, 20 mL was measured and poured into the 35 mL vial with approximately 1 cm of the solution above the sample. A magnetic stir bar was added and the vial was covered with a special lid designed to control pressure. The vials, lids, and stir bars were provided by CEM Corp. for specific use with the Discover S Class microwave.

Growth times were varied from 1 minute to 12 hours (720 min). Direct control of the process temperature at set temperatures between 70-100°C was achieved using the integrated infrared temperature control. For all runs a power limit of 50W was used. At the start of the run, the Discover S Class ramps to the set temperature with microwave power at the set limit. Once the set temperature WAS reached, power WAS REDUCED to near zero for the rest of the run. As described in more detail later, it was found that ramp time, temperature control, and power control critically depend on the performance of the lid.

The precursors ($Zn(NO_3)_2$ and HMT) were both varied in concentration ranging from 5 to 50 mM. $Zn(NO_3)_2$ to HMT concentration ratios included 1:1, 2:1 and 1:2. All samples were grown with the stirbar/agitation speed set to "low". After growth samples were immediately dried via wicking with Kimwipes. By visual inspection, samples appeared white with varying color across the sample.

For comparison, hydrothermal growth was also performed on a hot plate for 6 hours at 80°C in a solution of 250 mL DI water, 0.19 grams $Zn(NO_3)_2$ and 0.09 grams HMT.

A Leo 1560 scanning electron microscope (SEM) operated at an accelerating voltage of 3.00 kV or 5.00 kV with a working distance of 3 – 8 mm was used to access NW morphology (including length, diameter, density, growth orientation with respect to the substrate, tapering, and cross-sectional shape).

Prior to imaging, a thin carbon coating was applied to prevent image drift and charging. NW length, diameter, and angle with respect to normal were determined from the average of at least five wires from a cross sectional image. Error in THE measurements WAS dominated by uniformity across the sample, which is estimated at ± 8%, as discussed in the following section. All density measurements WERE based on the number of discernable wires that could be seen in a 1 μm^2 square of a top-down SEM image. To help ensure that the crystalline structures on the seed layer were not being counted as wires, an object was only counted as a wire if it appeared brighter than its surroundings. To obtain greater accuracy, the number of wires was counted in several smaller areas which were then multiplied to determine the density per μm^2. X-ray diffraction (XRD) analysis of selected seed layers on Si was performed using a Bruker D8 Discovery.

3. Results and Discussion

3.1 Nanowire Dimensions (Length, Diameter and Aspect Ratio)

3.1.1 Length vs. Time

In general, it was found that wire length increased with time. Shown in Figure 1 are plots of average length vs. growth time for various 1:1 solution concentrations and growth temperatures. NWs in Figure 1(a) were grown on 90 nm ALD ZnO seed layer films with an underlying 10 nm thick ALD Al_2O_3 buffer layer ($ZnO/Al_2O_3/Si$). NWs in Figure 1(b) were grown on 90 nm ALD ZnO seed layer films without any buffer layer. On both growth substrates, NW length increased with growth time. The presence of the underlying buffer layer does not appear to have a large impact on NW length. NWs of roughly similar length were grown on both substrates for both 85 °C / 25 mM and 70°C / 25 mM conditions. Maximum length appears to be limited to about 1 μm. At an extremely long growth time of 12 hours, the 70°C / 25 mM NWs grew to 900 nm.

For growth times up to 60 min, growth at 85 °C produces longer wires than growth at 70°C. Growth at 100°C / 25 mM (not shown) produced wires of similar length to those grown under 85 °C / 25 mM conditions. However, due to reasons discussed below, process control at 100°C was poor and therefore strong conclusions cannot be drawn about growth saturation at higher temperature. Finally, NW length did not increase with time for the 5 mM solution, suggesting that the low solution concentration is limiting growth.

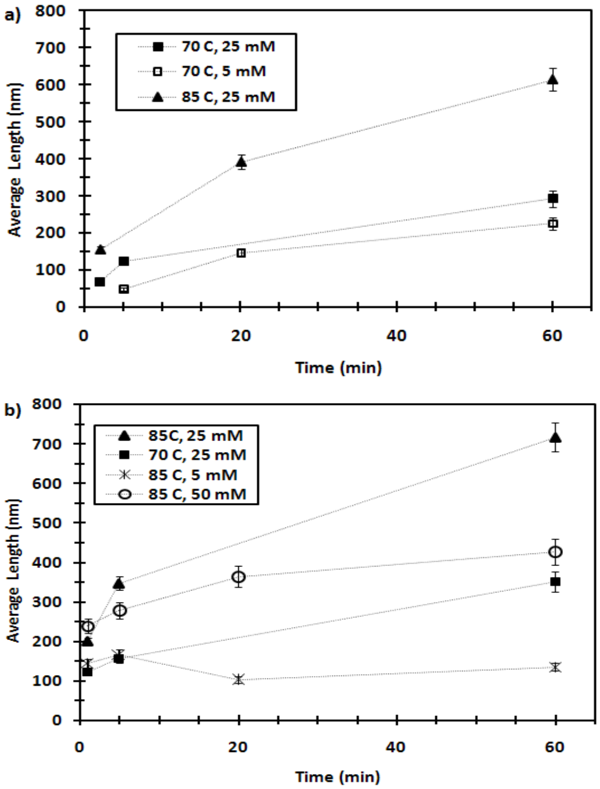

Figure 1: Plot of average NW length vs. growth time for ZnO NWs grown using various combinations of temperature and precursor concentration on either (a) 90 nm ALD ZnO films with a 10 nm thick Al_2O_3 buffer layer ($ZnO/Al_2O_3/Si$) or (b) 90 nm ALD ZnO films on Si. Lines are to guide the eye.

Shown in Figure 2 are a series of representative top down and cross sectional SEM images that illustrate NW growth as a function of time. All NWs were grown on $ZnO/Al_2O_3/Si$ substrates using a 25 mM (1:1) solution at 85 °C. The top-down image in Figure 2(b) makes it appear that the diameter of the wires is changing, but the NWs in this sample were tapered (as shown in cross-section) because of process control issues described later.

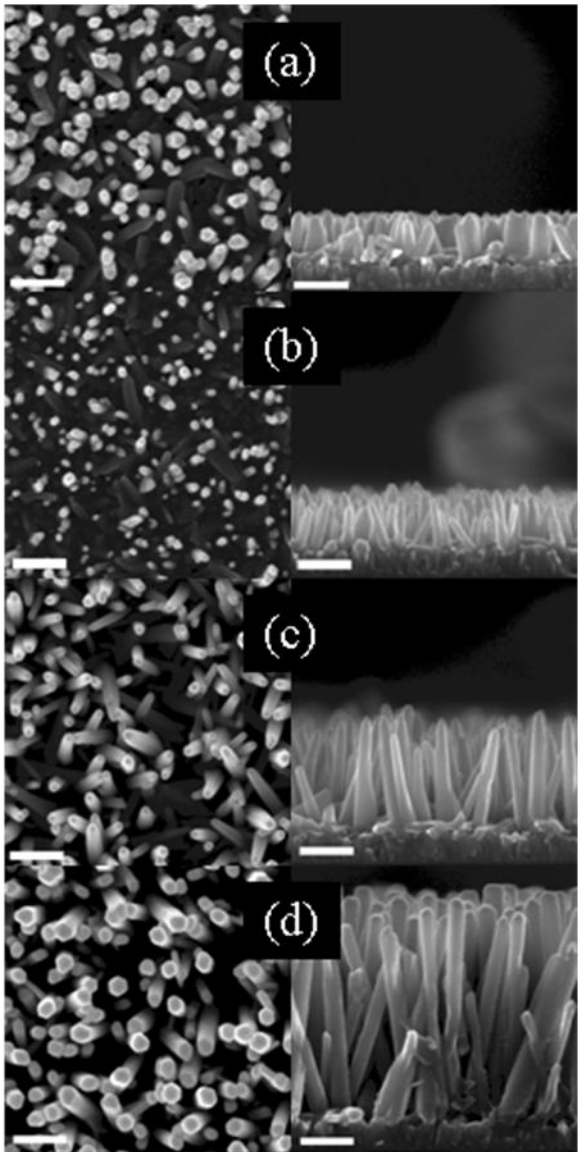

Figure 2: SEM images illustrating NW growth on $ZnO/Al_2O_3/Si$ substrates using a 25 mM (1:1) solution at 85 °C after (a) 1 min, (b) 5 min, (c) 20 min, and (d) 60 min of growth time. The scale bars shown for the top-down

images are 100 nm. For the cross-sectional images, the scale bar shown is 200 nm.

3.1.2 Length vs. Concentration

In Figure 3 we show that when the ratio between precursors is held constant at 1:1, the length of the wires is at a maximum at 25 mM. The growths represented in this figure were grown on either 90 nm ALD ZnO films with 10 nm thick Al_2O_3 buffer layers ($ZnO/Al_2O_3/Si$) or 90 nm ALD ZnO films on Si. For both ZnO/Si and $ZnO/Al_2O_3/Si$ seed layers, average NW length is seen to increase with 1:1 solution concentration until the 25 mM point. The average length of both the 70°C and 85 °C growths conducted at 50 mM is actually shorter than the average length at 25 mM, suggesting saturation of the growth rate above 25 mM 1:1 solution concentration and that perhaps too much HMT limits the reaction, as suggested by [8]. It is also seen that for 5 mM concentration, the growth rate is small, suggesting that the low concentration is limiting the deposition rate. This is consistent with the 85 °C, 5 mM growth shown in Figure 1(b), which shows little change in length over time.

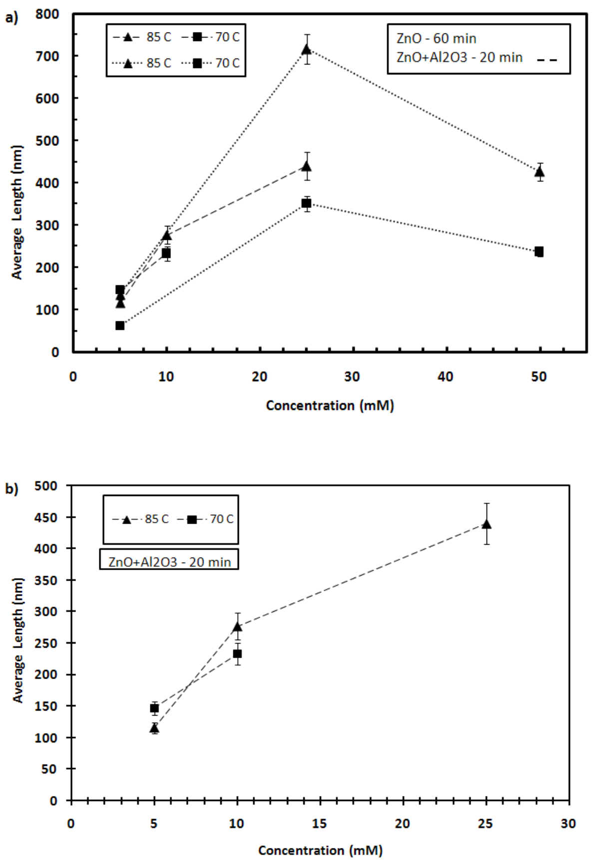

Figure 3: Plot of length vs. 1:1 precursor concentration for NWs that were grown for (a) 60 minutes on 90 nm ALD ZnO films on Si and (b) 20 minutes on 90 nm ALD ZnO films with a 10 nm thick Al_2O_3 buffer layer ($ZnO/Al_2O_3/Si$). Dashed lines are to guide the eye.

The impact of the ratio between the $Zn(NO_3)_2$ and HMT concentrations was also investigated. Figure 4 shows that the dependence of the lengths of the wires on this concentration ratio. The ratio of the precursors affected the NW length; this is clearly apparent when the concentration ratio was 1:2. The HMT was expected to help the solution become more basic and help the formation of the ZnO nanowires, but as mentioned in [10], it is possible that only a certain minimum amount of HMT is needed for the growth process.

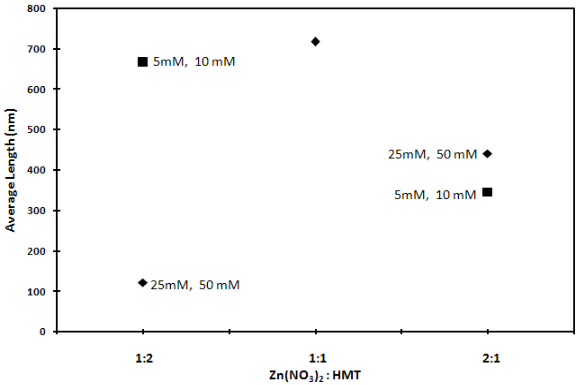

Figure 4: Plot of NW length vs. concentration ratio for various precursor concentrations.

3.1.3 Longest wires

Maximum length appears to be a limitation of the microwave hydrothermal growth method. For a reasonable growth time of 60 minutes, the longest wires achieved on a 90 nm ZnO seed layer were 696 nm long, using a 25 mM solution (1:1 concentration ratio) at 85 °C. For a thicker 200 nm ZnO seed layer wires up to 1 µm in length were obtained using the same growth conditions. Using the same growth conditions on a 90 nm ZnO/Al_2O_3/Si substrate, the maximum length obtained in 60 minutes was 821 nm. Even for an overnight growth, the maximum length achieved was less than 1 µm. However, there are still applications for short nanowires, such as growth on Kevlar for energy harvesting applications [11].

3.1.4 Diameter

For a given substrate, the NW diameter does not appear to be a strong function of time, temperature, or concentration. For all growths on 90 nm ALD ZnO seed layers, the average NW diameter was 70±6 nm. However, as discussed below, the morphology of the seed layer was found to have a strong impact on NW diameter.

3.1.5 Aspect ratio

Due, in part, to the weak dependence of NW diameter on time and other process variables, it was found that aspect ratio (length over diameter) of the NWs did not have a strong dependence on precursor concentration or growth temperature. Shown in Figure 5 is a plot of the average aspect ratio for NWs grown under various conditions on a ZnO/Al_2O_3/Si substrate. Within a single set of run conditions, it was seen that aspect ratio tends to increase with time, implying that wire length increases at a faster rate than wire diameter. Since the wires were typically the same diameter, no matter the growth conditions, process parameters that produced longer wires also typically had a higher aspect ratio. For all conditions investigated for a 1 hour or less growth time, the maximum aspect ratio obtained was ~13. This aspect ratio was obtained using 90 nm ALD ZnO seed layer with a 10 nm buffer layer, 85°C growth temperature, 60 minute growth time and a concentration ratio of 1:1 with a 25 mM concentration.

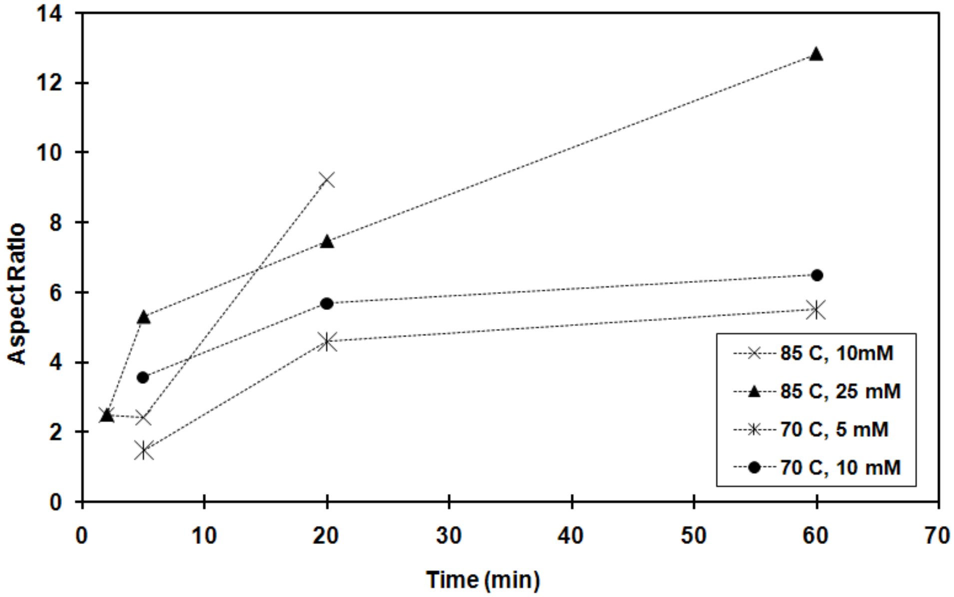

Figure 5: Aspect ratio as a function of growth time for NWs grown on 10 nm buffer alumina, 90 nm ZnO.

The diameter of NWs grown on ZnO seed layers with an Al_2O_3 buffer layer was ~45±17 nm, thinner than NWs grown on ZnO seed layer films deposited directly on Si, which were ~70 nm. However, since the wires which were grown on substrates with the Al_2O_3 buffer layer were also typically shorter, other than for optimal growth conditions, than those without the buffer layer, the aspect ratio is not significantly different.

3.2 Density

NW density (number of NWs / **µm**) did not appear to be strongly dependent on precursor concentration, time, or temperature. Typical top-down SEM images indicating NW density are shown in Figure 2. An average density of 180 NWs / **µm**± 90 NWs / **µm** was observed for all runs on 90 nm ALD ZnO seed layers, with or without buffer layers. There was not a distinct change in density with the addition of an alumina buffer layer. Note that since all analysis was performed manually from analysis of top down SEM images, and since the counting of wires in these images is somewhat subjective (see Figure 2), wire density results have a high variation.

3.3 Orientation

For all growths performed, NWs were found be oriented roughly perpendicular to the surface with an average angle from normal of 6° ±5°. Wire orientation was not found to be strongly dependent upon precursor concentration, growth temperature, or time.

3.4 Seed layers, diameter, morphology

Figure 6 shows top-down and cross-sectional images for growth on a variety of seed layers. It was found that the seed layer had a strong impact on wire morphology. Extremely thick wires resulted from growth on 90nm ZnO that had been annealed at 900°C either in N_2 or air. For example, for N_2 annealed samples, wires produced were almost 400 nm in diameter and over a 1000 nm tall. The 900°C seed layer anneal ambient also had an impact on NW morphology. As shown in 7(c) and 7(e) NWs annealed in O_2 were found to be more tapered than those grown in N_2.

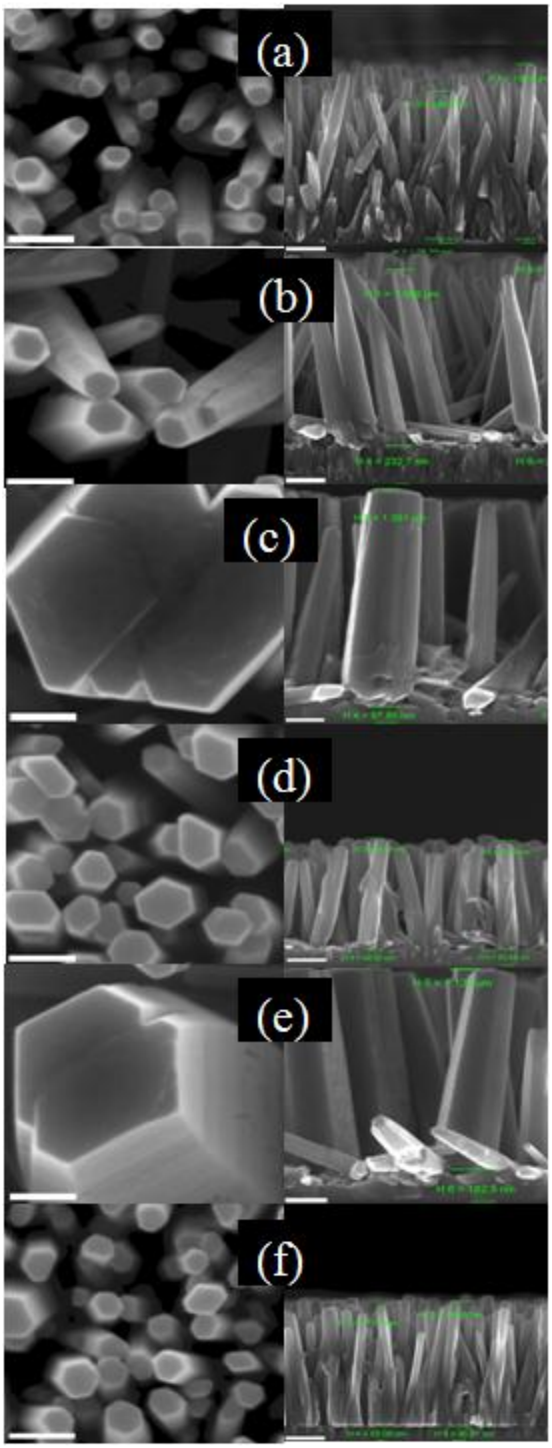
(a)
(b)
(c)
(d)
(e)
(f)

Figure 6: SEM images of growth on (a) 15 nm thick ALD ZnO seed layer, (b) 200 nm thick ALD ZnO seed layer, (c) 90 nm ALD ZnO seed layer annealed in N_2 at 900°C, (d) 90 nm ALD ZnO seed layer annealed in N_2 at 400°C, (e) 90 nm ALD ZnO seed layer annealed in air at 900°C and (f) 90 nm sputtered ZnO. The scale bars shown for the top-down images are 100 nm long, and the scale bars for the cross-sectional images are 200 nm.

X-ray diffraction was used to analyze selected ZnO films. Figure 7 shows four scans performed from 30 to 37 in 2θ with a step size of 0.01. Data are vertically offset for ease of visualization. There is little structural difference between the 90 nm ZnO seed layer and the seed layer which has a 10 nm buffer layer of Al_2O_3. When a high temperature anneal was included as part of the seed treatment prior to growth, the film crystallinity increased, as expected. The films with greater crystallinity corresponded to growth of NWs with a larger diameter. Also, a secondary phase was formed during this high temperature anneal. Given the material present and the location of the anomalous diffraction peak, it is likely that the second phase is Zn_2SiO_4. The relative intensities of the ZnO *c*-axis peak and the anomalous peak also indicate that an oxidizing environment promotes the formation of zinc silicate at the expense of crystalline ZnO; the contrary is true in a reducing environment (as expected). Since the Zn_2SiO_4 phase is likely formed at the interface between the ZnO seed layer and the Si substrate, the increased diameter of the NWs grown on annealed layers is likely due to the increase in the average crystallite size which seeds NW growth. These results demonstrate the strong influence that seed layer morphology has on NW morphology [17] even at low temperature.

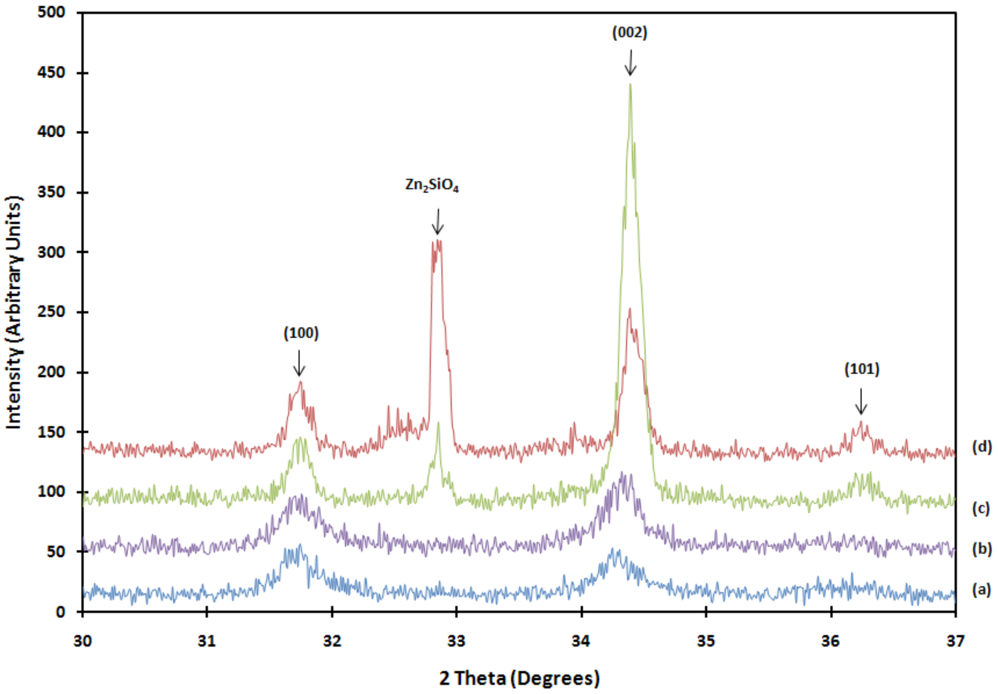

Figure 7: XRD data showing crystalline peaks for (a) 90 nm ALD ZnO as deposited (b) 10 nm ALD Al_2O_3 buffer, 90 nm ZnO seed layer as deposited, (c) 90 nm ALD ZnO annealed in N_2 and (d) 90 nm ALD ZnO annealed in O_2.

3.5 Crystallites

One of the problems encountered with hydrothermal growth using a hot plate is the undesirable homogeneous nucleation and growth of crystallites in the bulk of the solution and subsequent deposition on the growth substrate [10]. SEM images comparing hydrothermal growth using either (a) a hot plate or (b) the microwave as the heating mechanism are shown in Figure 2. The crystallites indicated in (a) are 2-4 µm long and approximately 300 nm wide. The crystallites appeared in nearly every run performed using a hot plate, whereas no large crystallites were found in any of the microwave runs that exhibited good process control.

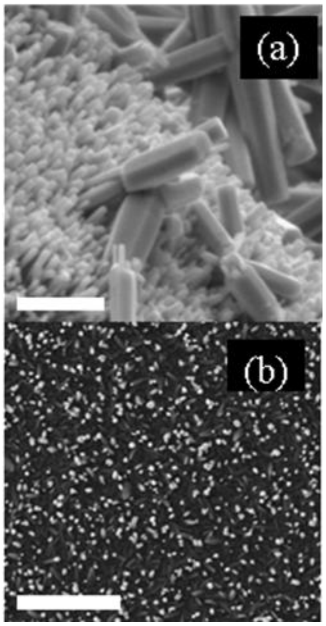

Figure 8: Hot plate growths had additional crystallites which covered the surface of the sample as shown in (a), well controlled microwave growths were free of unwanted crystallites as shown in (b). The scale bars are 1 µm in length.

3.6 Process Control

NW morphology, length, and uniformity were found to be a strong function of microwave process control. Process control in this microwave system was found to depend on the performance of the pressure control lid. When the lid performed well, pressure was maintained and the process was well controlled. The system ramped to the maximum set temperature in a fairly constant amount of time and achieved the maximum set temperature without overshoot. After reaching the maximum temperature, the temperature was held steady throughout the run with little power input. With good process control, good NW length uniformity was achieved and NW length was found to be a well-behaved function of time, precursor concentration, temperature, and seed layer structure.

On the other hand, if the lid did not seal completely, pressure in the vial was not maintained. The lack of pressure control allowed evaporation from the vial and cooling, resulting in an increase in the amount of time it takes to ramp to maximum temperature, overshoot of the maximum temperature, and fluctuation of the power and the temperature after the maximum temperature is reached. These poorly controlled runs resulted in shorter NWs with poor across-sample uniformity, and loss of strong hexagonal structure.

Figure 9 shows representative SEM images for NWs grown for 60 minutes at 85 °C / 25 mM for (a) good, (b) poor, and (c) medium process control. As shown in Figure 9(a), for the NWs grown with good process control, the average NW length was 696 nm ± 7%, despite visible non-uniformity of the samples (variation of the surface color (blue to pink) and coverage by white powder). In contrast, when the process was poorly controlled (Figure 9(b)), the NW length was only 242 nm with ± 30% variation across the sample. These NWs were much shorter than those produced in a well-controlled run. In addition, the morphology of the NWs was different for well-controlled and for poorly controlled runs. As seen in (b), the NWs produced in a poorly controlled run were more tapered than the NWs produced in the well-controlled run (a). Lastly, shown in (c) are images of a run in which parameter control was intermediate between (a) and (b) resulting in NWs that were 740 nm long ± 17% across the sample. We found that reused lids almost always exhibited poor control. In addition, approximately 1 out of 5 new lids also exhibited poor pressure control.

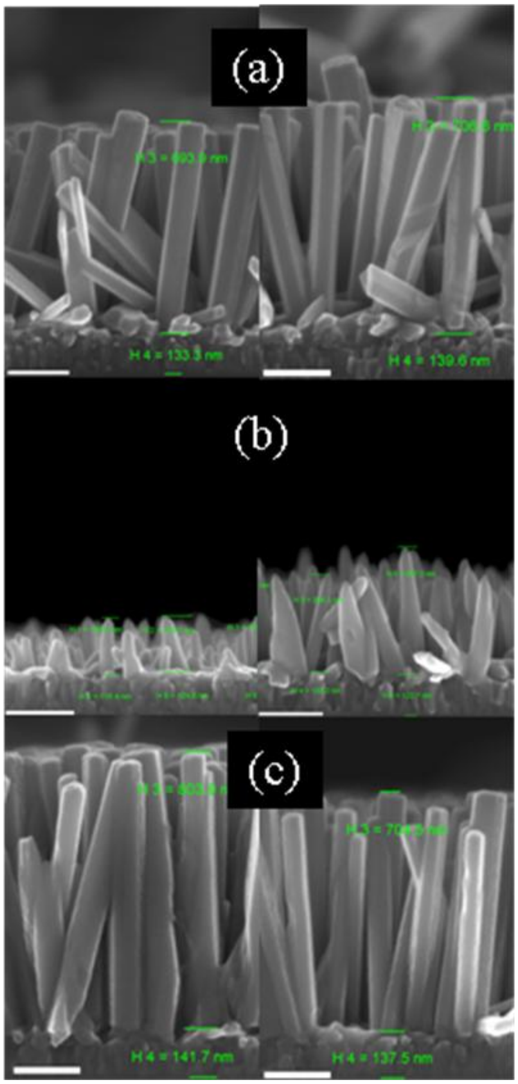

Figure 9: Process control affects on morphology, (a) well-controlled growth with consistent wire lengths and uniformity across the sample, (b) poorly controlled growth with altered morphology and wide variation in length and (c) a moderately well-controlled growth. Scale bars shown are all 200 nm in length.

4. Summary

ZnO NWs were grown via a hydrothermal method using a Discover S Class microwave with an integrated IR temperature controller. Specialized lids, vials and stirbars were used for experiments. The influence of growth temperature, growth time, solution concentration, and seed layer crystallinity on ZnO NW length, diameter, aspect ratio, growth orientation, density, and morphology was investigated. The seed layer upon which the NWs were grown influenced the resulting NW morphology more than any other variable in this work. Annealing at 900°C in either air, or N_2, increased the seed layer crystallinity which, in turn, increased the NW diameter, suggesting a quasi-epitaxial growth of the NWs. It was found that the microwave oven was capable of achieving very good control of the growth. When lids sealed completely and pressure was well controlled within the vial, vertically-oriented NWs with lengths 696 nm ± 7% were obtained for 25 mM, 1:1 ratio of precursors, at a growth temperature of 85 °C and growth time of 60 minutes. These wires are similar in length to those used in [18] for their piezoelectric-inspired device. The uniformity across the sample will help ensure a larger number of contacts to the NWs and more consistent bending in each NW.

ACKNOWLEDGEMENTS

The authors would like to thank the Office of Naval Research (N00014-07-1-0457), the Army Research Laboratories (W911NF-07-2-0083), the Oregon

Nanoscience and Microtechnologies Institute, the National Science Foundation (NSF DMR REU- 0805372), the Intel Scholars Programs, and the Tektronix Scholars Program for support of this work. The authors also thank S. DeHan and CEM Corporation for loan of the Discover microwave, Dr. B. Gibbons (OSU) and R. Ravichandran (OSU) for assistance with XRD, and Todd Waggoner (OSU) for assistance with seed layer deposition, and HP for **use of SEM for Figure xx.**

REFERENCES

[1] J. Cheng, X. Zhang, and Z. Luo, "Aligned ZnO nanorod arrays fabricated on Si substrate by solution deposition," *Physica E: Low-dimensional Systems and Nanostructures,* vol. 31, Mar. 2006, pp. 235-239.

[2] H.J. Fan, W. Lee, R. Hauschild, M. Alexe, G. Le Rhun, R. Scholz, A. Dadgar, K. Nielsch, H. Kalt, A. Krost, M. Zacharias, and U. Gosele, "Template-Assisted Large_Scale Ordered Arrays of ZnO Pillars for Optical and Piezoelectric Applications," *Small,* vol. 2, Apr. 2006, pp. 561-568.

[3] L.E. Greene, B.D. Yuhas, M. Law, D. Zitoun, and P. Yang, "Solution-Grown Zinc Oxide Nanowires," *Inorganic Chemistry,* vol. 45, Sep. 2006, pp. 7535-7543.

[4] M.H. Huang, Y. Wu, H. Feick, N. Tran, E. Weber, and P. Yang, "Catalytic Growth of Zinc Oxide Nanowires by Vapor Transport," *Advanced Materials*, vol. 13, Jan. 2001, pp. 113-116.

[5] Q. Li, V. Kumar, Y. Li, H. Zhang, T.J. Marks, and R.P.H. Chang, “Fabrication of ZnO Nanorods and Nanotubes in Aqueous Solutions,” *Chemistry of Materials*, vol. 17, Feb. 2005, pp. 1001-1006.

[6] Y. Tong, Y. Liu, L. Dong, D. Zhao, J. Zhang, Y. Lu, D. Shen, and X. Fan, “Growth of ZnO Nanostructures with Different Morphologies by Using Hydrothermal Technique,” *Journal of Physical Chemistry*, vol. 110, Sep. 2006, pp. 20263-20267.

[7] L. Vayssieres, “Growth of Arrayed Nanorods and Nanowires of ZnO from Aqueous Solutions,” *Advanced Materials*, vol. 15, Mar. 2003, pp. 464-466.

[8] S. Xu, C. Lao, B. Weintraub, and Z.L. Wang, “Density-controlled growth of aligned ZnO nanowire arrays by seedless chemical approach on smooth surfaces,” *Journal of Materials Research*, vol. 23, Aug. 2008, pp. 2072-2077.

[9] G.D. Yuan, W.J. Zhang, J.S. Jie, X. Fan, J.A. Zapien, Y.H. Leung, L.B. Luo, P.F. Wang, C.S. Lee, and S.T. Lee, “p-Type ZnO Nanowire Arrays,” *Nano Letters*, vol. 8, Apr. 2008, pp. 2591-2597.

[10] A.D. Mason, T.J. Waggoner, S.W. Smith, J.F. Conley Jr., B.J. Gibbons, D. Price, and D. Allman, “Hydrothermal Synthesis of Zinc Oxide Nanowires on Kevlar using ALD and Sputtered ZnO Seed Layers,” *Material Research Society Symposium Proceedings*, vol. 1178, 2009, pp. 1-6.

[11] Y. Qin, X. Wang, and Z.L. Wang, “Microfibre-nanowire hybrid structure for energy scavenging,” *Nature,* vol. 451, Feb. 2008, pp. 809-813.

[12] H.E. Unalan, P. Hiralal, N. Rupesinghe, S. Dalal, W.I. Milne, and G.A.J. Amaratunga, “Rapid synthesis of aligned zinc oxide nanowires,” *Nanotechnology*, vol. 19, May. 2008, pp. 1-5.

[13] P. Chang and C. Chien, “Finite size effect in ZnO nanowires,” *Applied Physics Letters*, vol. 90, Mar. 2007, pp. 1-3.

[14] W. Yang, F. Wan, S. Chen, and C. Jiang, “Hydrothermal Growth and Application of ZnO Nanowire Films with ZnO and TiO2 Buffer Layers in Dye-Sensitized Solar Cells,” *Nanoscale Research Letters,* vol. 4, Dec. 2009, pp. 1486-1492.

[15] D. Kang, S.K. Han, J. Kim, S.M. Yang, J.G. Kim, S. Hong, D. Kim, and H. Kim, “ZnO nanowires prepared by hydrothermal growth followed by chemical vapor deposition for gas sensors,” *Journal of Vacuum Science and Technology*, vol. 27, May. 2009, pp. 1667-1672.

[16] S. Baruah, C. Thanachayanont, and J. Dutta, “Growth of ZnO nanowires on nonwoven polyethylene fibers,” *Science and Technology of Advanced Materials*, vol. 9, Jun. 2008, pp. 1-8.

[17] J.F. Conley Jr., L. Stecker, and Y. Ono, “Directed assembly of ZnO nanowires on a Si substrate without a metal catalyst using a patterned ZnO seed layer,” *Nanotechnology*, vol. 16, Jan. 2005, pp. 292-296.

[18] M.-Y. Choi, D. Choi, M.-J. Jin, I. Kim, S.-H. Kim, J.-Y. Choi, S.Y. Lee, J.M. Kim, S.-W. Kim, “Mechanically Powered Transparent Flexible Charge-Generating Nanodevices with Piezoelectric ZnO Nanorods,” *Advanced Materials*, vol 21., 2009, pp. 2185-2189.

FIGURE CAPTIONS

Figure 1: Plot of average NW length vs. growth time for ZnO NWs grown using various combinations of temperature and precursor concentration on either (a) 90 nm ALD ZnO films with a 10 nm thick Al_2O_3 buffer layer ($ZnO/Al_2O_3/Si$) or (b) 90 nm ALD ZnO films on Si. Lines are to guide the eye.

Figure 2: SEM images illustrating NW growth on $ZnO/Al_2O_3/Si$ substrates using a 25 mM (1:1) solution at 85 °C after (a) 1 min, (b) 5 min, (c) 20 min, and (d) 60 min of growth time. The scale bars shown for the top-down images is 100 nm. For the cross-sectional images, the scale bar shown is 200 nm.

Figure 3: Plot of length vs. 1:1 precursor concentration for NWs that were grown for (a) 60 minutes on 90 nm ALD ZnO films on Si and (b) 20 minutes on

90 nm ALD ZnO films with a 10 nm thick Al_2O_3 buffer layer ($ZnO/Al_2O_3/Si$). Dashed lines are to guide the eye.

Figure 4: Plot of NW length vs. concentration ratio for various precursor concentrations.

Figure 5: Aspect ratio as a function of growth time for NWs grown on 10 nm buffer alumina, 90 nm ZnO.

Figure 6: SEM images of growth on (a) 15 nm thick ALD ZnO seed layer, (b) 200 nm thick ALD ZnO seed layer, (c) 90 nm ALD ZnO seed layer annealed in N_2 at 900°C, (d) 90 nm ALD ZnO seed layer annealed in N_2 at 400°C, (e) 90 nm ALD ZnO seed layer annealed in air at 900°C and (f) 90 nm sputtered ZnO. The scale bars shown for the top-down images are 100 nm long, and the scale bars from the cross-sectional images are 200 nm.

Figure 7: XRD data showing crystalline peaks for (a) 90 nm ALD ZnO as deposited (b) 10 nm ALD Al_2O_3 buffer, 90 nm ZnO seed layer as deposited, (c) 90 nm ALD ZnO annealed in N_2 and (d) 90 nm ALD ZnO annealed in O_2.

Figure 8: Hot plate growths had additional crystallites which covered the surface of the sample as shown in (a), well controlled microwave growths were free of unwanted crystallites as shown in (b). The scale bars are 1 µm in length.

Figure 9: Process control affects on morphology, (a) well-controlled growth with consistent wire lengths and uniformity across the sample, (b) poorly

controlled growth with altered morphology and wide variation in length and (c) a moderately well-controlled growth. Scale bars shown are all 200 nm in length.